

ARTICLE

Induction and inhibition of the pan-nuclear gamma-H2AX response in resting human peripheral blood lymphocytes after X-ray irradiation

D Ding¹, Y Zhang¹, J Wang¹, X Zhang¹, Y Gao¹, L Yin¹, Q Li¹, J Li² and H Chen¹

Human peripheral blood lymphocytes (HPBLs) are one of the most sensitive cells to ionizing radiation (IR) in the human body, and IR-induced DNA damage and functional impairment of HPBLs are the adverse consequences of IR accidents and major side effects of radiotherapy. Phosphorylated H2AX (γ H2AX) is a sensitive marker for DNA double-strand breaks, but the role and regulation of the pan-nuclear γ H2AX response in HPBLs after IR remain unclear. We herein demonstrated that the pan-nuclear γ H2AX signals were increased in a time- and dose-dependent manner, colocalized with > 94% of TUNEL apoptotic staining, and displayed a typical apoptotic pattern in resting HPBLs after low LET X-ray IR. In addition, the X-irradiation-induced pan-nuclear p-ATM and p-DNA-PKcs responses also occurred in resting HPBLs, and were colocalized with 92–95% of TUNEL staining and 97–98% of the pan-nuclear γ H2AX signals, respectively, with a maximum at 6 h post irradiation, but disappeared at 24 h post irradiation. Moreover, ATM/DNA-PKcs inhibitor KU55933, p53 inhibitor PFT- μ and pan-caspase inhibitor ZVAD-fmk significantly decreased X-irradiation-induced pan-nuclear γ H2AX signals and TUNEL staining, protected HPBLs from apoptosis, but decreased the proliferative response to mitogen in X-irradiated HPBLs. Notably, whereas both KU55933 and PFT- μ increased the IR-induced chromosome breaks and mis-repair events through inhibiting the formation of p-ATM, p-DNA-PKcs and γ H2AX foci in X-irradiated HPBLs, the ZVAD-fmk did not increase the IR-induced chromosomal instability. Taken together, our data indicate that pan-nuclear γ H2AX response represents an apoptotic signal that is triggered by the transient pan-nuclear ATM and DNA-PKcs activation, and mediated by p53 and pan-caspases in X-irradiated HPBLs, and that caspase inhibitors are better than ATM/DNA-PKcs inhibitors and p53 inhibitors to block pan-nuclear γ H2AX response/apoptosis and protect HPBLs from IR.

Cell Death Discovery (2016) 2, 16011; doi:10.1038/cddiscovery.2016.11; published online 21 March 2016

INTRODUCTION

In coping with ionizing radiation (IR)-induced double strand breaks (DSBs), mammalian cells promptly initiate the DNA damage response (DDR) to ensure efficient and accurate repair of damaged DNA and cell survival.¹ It is commonly believed that a key step in the response to DSBs is histone variant H2AX phosphorylation at serine 139 (S139) in the megabase chromatin region flanking the break to provide a docking site for DNA repair factors, which form visible γ H2AX immunofluorescent foci in mammals.^{2,3} Ataxia telangiectasia mutated (ATM) and DNA-dependent protein kinase catalytic subunit (DNA-PKcs) are two primary kinases that phosphorylate H2AX at S139 in response to IR-induced DSBs.^{4–6} Moreover, ATM also phosphorylates and activates the tumor suppressor p53 to induce cell cycle arrest, DNA repair or apoptosis by transactivating downstream target genes,^{7,8} and DNA-PKcs is dispensable for p53 activation.^{9–13} In addition to its role in transcription regulation, p53 also functions in a transcriptionally independent manner in DNA repair¹⁴ and apoptosis.^{15,16} The activation of the caspase family of cysteine proteases has been shown as an extremely important step in the execution of p53-mediated transcription-dependent and -independent apoptosis.¹⁷

Apart from IR-induced formation of γ H2AX foci, the induction of pan-nuclear γ H2AX signals has been demonstrated as a cellular reaction to IR and as a consequence of various regulation

mechanisms.^{18–20} Cook *et al.*¹⁸ have reported that H2AX phosphorylation at tyrosine 142 (Y142) induces an apoptotic response instead of a damage repair response to genotoxic stress by preventing the binding of the damage repair factors to phospho-serine 139 of γ H2AX and promoting the effective recruitment of pro-apoptotic factors to H2AX. Moreover, H2AX phosphorylation at Y142 produces visible whole-nuclear γ H2AX immunofluorescence staining instead of foci in TUNEL-positive mouse embryonic fibroblasts exposed to 100 Gy of irradiation.¹⁸ However, the relationship between pan-nuclear γ H2AX response and radiation quality remains unclear. Markova *et al.*¹⁹ observed the γ -irradiation-induced pan-nuclear γ H2AX response in HPBLs, but it was unknown whether the pan-nuclear γ H2AX response was related to apoptosis. In addition, it was demonstrated that localized heavy ion irradiation-induced clustered DNA damage in sub-nuclear regions induced the transient nuclear-wide H2AX phosphorylation in undamaged chromatin in mammalian cells, including human fibroblasts, the U2-OS tumor cells, mouse embryonic fibroblast cells and hamster ovary cells; however, none of the neighboring un-irradiated cells showed a nuclear-wide γ H2AX response, and targeted cytoplasmic irradiation with particles also did not induce the nuclear-wide γ H2AX response.²⁰ It has been proposed that the particle-induced pan-nuclear γ H2AX response is caused by ATM and DNA-PK activity distant to sites of

¹Department of Radiation Biology, Institute of Radiation Medicine, Fudan University, Shanghai, China and ²Clinical Department at Renji Hospital, Shanghai Jiao Tong University School of Medicine, Shanghai, China.

Correspondence: H Chen (E-mail: hhchen@shmu.edu.cn)

Received 13 January 2016; accepted 17 January 2016; Edited by I Harris

DNA damage and is not related to either apoptosis or DSB repair.²⁰ The nuclear-wide kinase activity of ATM and DNA-PK may be elicited by dense IR-induced small DNA fragments²¹ or by diffusion of active kinases from DNA DSBs. In addition, pan-nuclear γ H2AX signals were induced by other stressors via various regulation mechanisms. It has been reported that tumor necrosis factor-related apoptosis-inducing ligand (TRAIL), staurosporine, etoposide and ultraviolet irradiation induce the pan-nuclear γ H2AX response associated with apoptosis in human cancer cells,²² mouse fibroblasts, Chinese hamster ovary cells, human fibroblasts^{23–25} and resting human T cells.²⁶ The pan-nuclear γ H2AX response can be caused by replication-mediated DSBs in cancer cells treated with camptothecin,²⁷ indenoisoquinolines²⁸ or gemcitabine,²⁹ which are not related to apoptotic DNA fragmentation. Moreover, small DNA molecules, which mimic DNA DSBs (called D bait) and disorganize the DNA repair system in cancer cells,^{30,31} and adeno-associated virus replication in infected host cells, which could be explained as a reaction to the single-stranded DNA part of the virus that compromises DNA repair, also can induce the pan-nuclear γ H2AX response.^{32,33} The changes in chromatin structure after hypotonic treatment are sufficient to elicit extensive pan-nuclear γ H2AX formation in the absence of DNA strand breaks, which are not related to apoptosis.³⁴

Human peripheral blood lymphocytes (HPBLs) are extremely sensitive to IR and represent the most common target cells for biological dosimetric,³⁵ radiosensitive³⁶ and immune function studies.^{37,38} γ H2AX foci have been shown to be the most sensitive dosimeter and radiosensitive indicator.³⁹ HPBLs are non-dividing cells in the G0 phase of the cell cycle, and can proliferate to generate the immune response if stimulated. Therefore, HPBLs are able to efficiently repair DSBs to prevent apoptosis and mutations. Low LET γ -ray irradiation induces the activation of DDR proteins through phosphorylation of ATM at Ser 1981, DNA-PKcs at tyrosine 2609 and H2AX at Ser 139 to form DNA repair foci in HPBLs.^{19,40,41} If the DNA damage is not repaired after IR, HPBLs undergo p53-dependent apoptosis through the caspase

cascade,^{42–47} and subsequently, functional inhibition of HPBLs may result in immune suppression in individuals exposed to acute or chronic IR at high doses and in radio/chemotherapy patients.^{48,49} Therefore, it is of interest to understand the relationships among pan-nuclear γ H2AX signals, apoptosis, DSB repair, chromosomal aberration and proliferative function in resting HPBLs exposed to low LET X-irradiation, and to explore the pharmacological approaches to protect HPBLs against IR-induced pan-nuclear γ H2AX response/apoptosis. In this study, we demonstrated that X-ray-induced pan-nuclear γ H2AX response represents an apoptotic signal in resting HPBLs, and is mediated by transient pan-nuclear ATM and DNA-PKcs activation and dependent on p53 and caspase activation. Our studies suggest that caspase inhibitors are better than ATM/DNA-PKcs inhibitors and p53 inhibitors to block pan-nuclear γ H2AX response/apoptosis and protect HPBLs from IR.

RESULTS

The kinetic patterns of the pan-nuclear responses are different from that of the DDR foci in resting HPBLs after X-irradiation. As shown in Figure 1a, we detected the nuclear-wide γ H2AX, p-ATM and p-DNA-PKcs responses and the γ H2AX, p-ATM and p-DNA-PKcs foci in resting HPBLs after X-irradiation. Importantly, the kinetic patterns of the pan-nuclear responses are different from that of the DDR foci (Figure 1b). For the γ H2AX signals, although the percentages of pan-nuclear γ H2AX-positive cells increased steadily after X-irradiation, the frequencies of the γ H2AX foci peaked at 30 min after X-irradiation, decreased rapidly during 6 h post irradiation and was reduced to approximately 8% of the peak value at 24 h post irradiation (Figure 1b, left panel). For the p-ATM and p-DNA-PKcs signals, the kinetic patterns of the p-ATM and p-DNA-PKcs foci were similar to that of the γ H2AX foci, but the percentages of pan-nuclear p-ATM- and p-DNA-PKcs-positive cells peaked at 6 h post irradiation and decreased to zero at 24 h post irradiation (Figure 1b, middle and right panel). These data

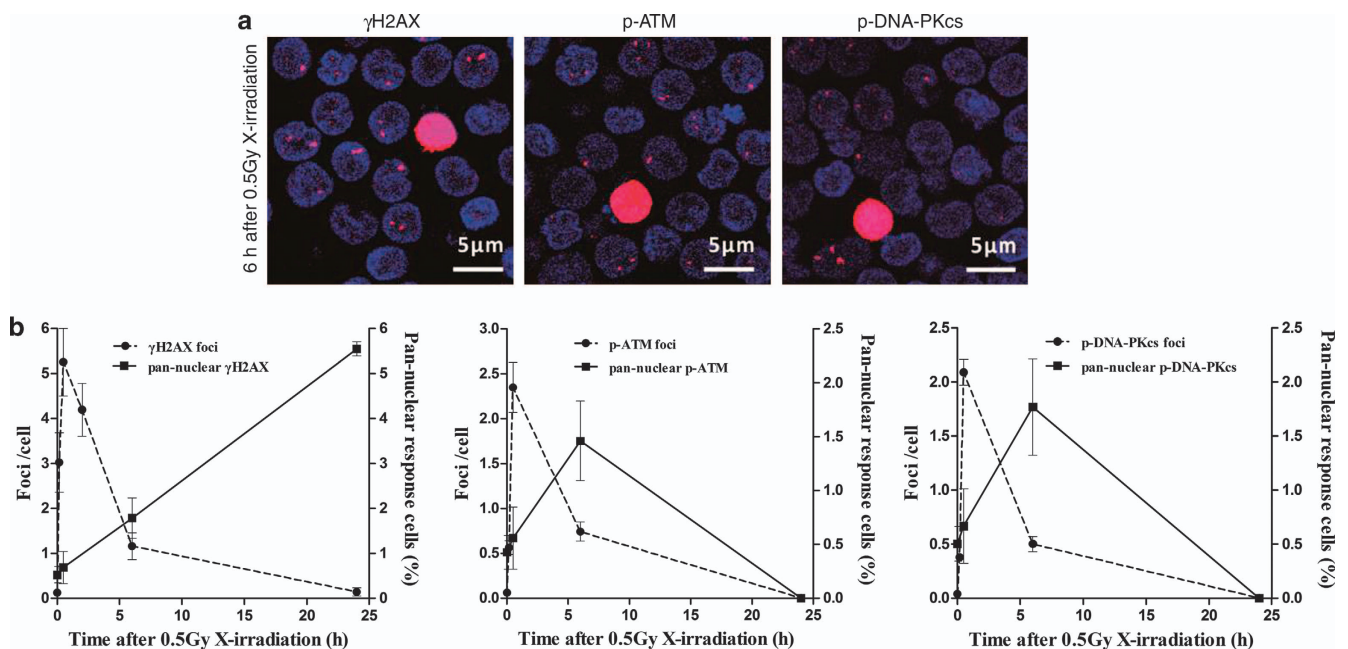


Figure 1. Distinct kinetic patterns between the pan-nuclear responses and the repair foci of γ H2AX, p-ATM and p-DNA-PKcs. (a) Representative images of X-irradiation-induced pan-nuclear signals and foci of γ H2AX, p-ATM and p-DNA-PKcs in resting HPBLs at 6 h after 0.5 Gy X-ray exposure. $\times 60$ magnification, $\times 1.0$ zoom. (b) HPBLs were irradiated with 0.5 Gy X-ray, and the pan-nuclear signals and foci of γ H2AX (left panel), p-ATM (middle panel) and p-DNA-PKcs (right panel) were examined at the indicated time points after irradiation and quantified by counting 1000–5000 HPBLs from each sample. γ H2AX, p-ATM and p-DNA-PKcs were labeled in red, and the nuclei were stained in blue with DAPI. Data are presented as the means \pm S.D. of four to six donors.

suggest that the nuclear-wide γ H2AX, p-ATM and p-DNA-PKcs responses are not related to DSB repair in resting HPBLs after X-irradiation.

X-irradiation-induced pan-nuclear γ H2AX, p-ATM and p-DNA-PKcs signals are colocalized with TUNEL apoptotic staining in resting HPBLs

It was reported that pan-nuclear formation of γ H2AX in undamaged chromatin induced by high-LET localized ion irradiation was not related to apoptosis in human fibroblasts, tumor cells and hamster ovary cells.²⁰ However, we found that the kinetics of the increase of the pan-nuclear γ H2AX response was similar to that of apoptotic induction at 0.5, 6 and 24 h post irradiation (0.5 or 5.0 Gy) in HPBLs. Moreover, the percentage of TUNEL-positive cells was similar to the percentage of pan-nuclear γ H2AX-positive cells at each time point after the same dose radiation (Figure 2a, left panel). More importantly, 94–99% of the TUNEL-positive cells also displayed pan-nuclear γ H2AX staining in a dose- and time-independent manner (Figure 2a, right panel; Figure 2c), indicating that pan-nuclear γ H2AX staining was associated with X-irradiation-induced apoptosis in resting HPBLs.

Furthermore, pan-nuclear p-ATM and p-DNA-PKcs signals were also colocalized with pan-nuclear γ H2AX or TUNEL staining at 6 h post irradiation in resting HPBLs. It was found that 93–95% of the TUNEL-positive cells also exhibited pan-nuclear p-ATM or p-DNA-PKcs staining at 6 h post irradiation (5 Gy) (Figures 2b and c). We further found that 97–98% of cells with pan-nuclear γ H2AX staining showed pan-nuclear p-ATM and p-DNA-PKcs staining (Figures 2b and c). Notably, HPBLs with pan-nuclear γ H2AX staining did not exhibit pan-nuclear p-ATM and p-DNA-PKcs staining at 24 h post irradiation (Figure 2c), suggesting that ATM and DNA-PKcs were only activated at early stages after irradiation.

According to the morphological signs of apoptosis progression such as apoptotic rings, pan-nuclear staining and apoptotic bodies, we observed three types of morphological characterization of the apoptotic γ H2AX response: γ H2AX ring versus TUNEL ring and very weak TUNEL pan-staining of the nucleus; pan-nuclear γ H2AX versus strong TUNEL pan-staining of the nucleus; and the γ H2AX pan-staining within apoptotic bodies. Notably, no DDR foci were observed in the pan-nuclear responses.

X-irradiation-induced pan-nuclear γ H2AX responses and apoptosis in resting HPBLs are mediated by ATM and DNA-PKcs

We next investigated the role of ATM and DNA-PKcs in nuclear-wide H2AX phosphorylation and apoptosis. It was found that pretreatment with KU55933, a potent inhibitor of ATM/DNA-PKcs, resulted in significant inhibition of X-irradiation-induced γ H2AX, p-ATM and p-DNA-PKcs focus formation at 30 min post irradiation (0.5 or 5 Gy) in resting HPBLs (Figure 3a), suggesting that KU55933 inhibited X-irradiation-induced DSB repair. In addition, KU55933 significantly inhibited the pan-nuclear p-ATM and p-DNA-PKcs signals at 6 h post irradiation (5 Gy) (Figure 3b, left panel) in HPBLs. The inhibitory effects of KU55933 on p-ATM and p-DNA-PKcs expression were also demonstrated by western blotting analysis (Figure 3b, right panel). We found that KU55933 also inhibited X-irradiation-induced p53 phosphorylation (Figure 3b, right panel). Correspondingly, KU55933 inhibited the pan-nuclear γ H2AX signals and TUNEL apoptosis at 6 and 24 h post irradiation (0.5 or 5 Gy) in resting HPBLs (Figure 3c). Together, our results suggest that KU55933 decreases X-irradiation-induced pan-nuclear γ H2AX responses and apoptosis by inhibiting transient pan-nuclear p-ATM and p-DNA-PKcs responses and p53 phosphorylation in resting HPBLs.

X-irradiation-induced pan-nuclear γ H2AX response and apoptosis in resting HPBLs were also mediated by p53 and pan-caspases

It has been shown that apoptosis of HPBLs is p53- and caspase-dependent.^{26,43–47} We next investigated the roles of p53 and caspases in nuclear-wide H2AX phosphorylation and apoptosis. It was found that pretreatment with the p53 inhibitor PFT- μ and pan-caspase inhibitor ZVAD-fmk significantly reduced X-irradiation-induced p53 phosphorylation and cleaved-caspase-3 expression in resting HPBLs (Figure 4a, left panel). Similar to the inhibitory effects of KU55933 on X-irradiation-induced pan-nuclear γ H2AX signals and TUNEL staining, pretreatment with PFT- μ or ZVAD-fmk also resulted in the significant suppression of X-irradiation-induced pan-nuclear γ H2AX signals and apoptosis at 24 h post irradiation (0.5 or 5 Gy) in resting HPBLs (Figure 4a, right panel), suggesting that p53 and caspases are involved in the regulation of the nuclear-wide γ H2AX response. Moreover, PFT- μ inhibited X-irradiation-induced pan-nuclear p-ATM and p-DNA-PKcs responses at 6 h post irradiation (5 Gy) and X-irradiation-induced p-ATM and p-DNA-PKcs focus formation at 4 h post irradiation, although it did not decrease X-irradiation-induced p-ATM and p-DNA-PKcs focus formation at 30 min post irradiation (Figure 4b), suggesting that p53 is involved in mediating the pan-nuclear p-ATM and p-DNA-PKcs responses, and has an important role in enhancing DSB repair in HPBLs after X-irradiation.

Effects of KU55933, PFT- μ and ZVAD-fmk on X-irradiation-induced chromosomal aberrations and proliferative response in resting HPBLs

Although KU55933, PFT- μ and ZVAD-fmk protect HPBLs from X-irradiation-induced apoptosis, it is not clear whether they affect X-irradiation-induced genomic instability and protect HPBLs function. Table 1 shows that X-irradiation significantly induced chromosomal aberrations including breaks, dicentric plus rings in resting HPBLs and increased the percentage of aberrant cells. KU55933 and PFT- μ , but not ZVAD-fmk, further significantly enhanced X-irradiation-induced chromosomal aberrations.

We investigated the impact of KU55933, PFT- μ and ZVAD-fmk on the proliferation of X-irradiated HPBLs. We found that the inhibitor (KU55933, PFT- μ or ZVAD-fmk) combined with X-irradiation resulted in a more significant decrease of the percentage of Ki67-positive cells than the inhibitor or X-irradiation alone in resting HPBLs, suggesting that KU55933, PFT- μ and ZVAD-fmk aggravated the inhibitory effect of X-irradiation on the proliferative response in resting HPBLs (Figures 5a–d).

DISCUSSION

Unlike the kinetics of localized ion-induced transient pan-nuclear γ H2AX response with a peak at \sim 1 h post irradiation, we demonstrated herein that X-irradiation-induced pan-nuclear γ H2AX response and apoptosis were increased in a dose- and time-dependent manner in resting HPBLs exposed to X-irradiation. This phenomenon is similar to the kinetics of the anticancer agent etoposide-induced pan-nuclear γ H2AX response and apoptosis in resting human T cells.²⁶ More importantly, we provide direct evidence that the X-irradiation-induced pan-nuclear γ H2AX response is presented in the apoptotic HPBLs. The apoptotic γ H2AX pan-nuclear response is a novel feature of the low LET IR-induced apoptosis in HPBLs, and could serve as a biomarker to distinguish apoptotic cells from the DNA-damaged cells with a focal pattern and to monitor the extent of radiation injury and side effects of radiotherapy.

In contrast, X-irradiation-induced pan-nuclear p-ATM and p-DNA-PKcs responses in resting HPBLs were transient with a maximum response at 6 h post irradiation and complete disappearance at 24 h post irradiation. The transient X-irradiation-

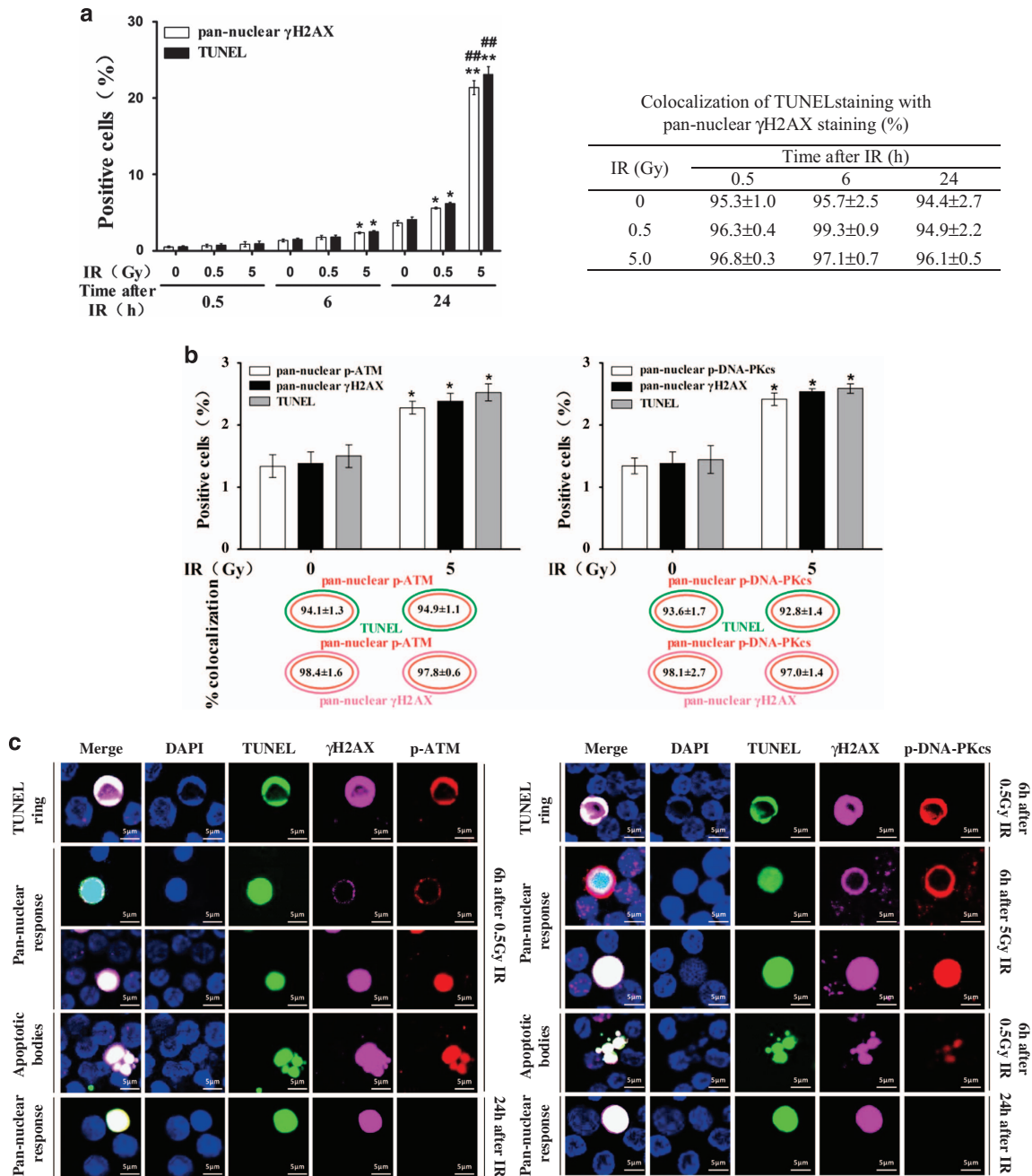


Figure 2. Relationship between pan-nuclear γ H2AX, p-ATM and p-DNA-PKcs responses and apoptosis in resting HPBLs exposed to X-ray irradiation. **(a)** HPBLs were irradiated with 0.5 and 5 Gy X-ray. The pan-nuclear γ H2AX, TUNEL-positive cells (left panel) and their colocalization (right panel) were examined at the indicated time points after irradiation. **(b)** HPBLs were irradiated with 5 Gy X-ray. The pan-nuclear p-ATM with the pan-nuclear γ H2AX and TUNEL-positive cells, pan-nuclear p-DNA-PKcs with the pan-nuclear γ H2AX and TUNEL-positive cells and their colocalization were examined at 6 h after irradiation. **(c)** Representative images of X-irradiation-induced pan-nuclear γ H2AX, p-ATM, p-DNA-PKcs and TUNEL staining and their colocalization in resting HPBLs at the indicated time points after irradiation. γ H2AX was labeled in infrared, p-ATM and p-DNA-PKcs in red and TUNEL in green, and nuclei were stained blue with DAPI. A total of 5000 HPBLs from each sample were examined to calculate the percentage of pan-nuclear γ H2AX, p-ATM, p-DNA-PKcs and TUNEL-positive cells. $\times 60$ magnification, $\times 1.0$ zoom. Data shown in panel **(a)** and panel **(b)** are presented as the means \pm S.D. of six donors. * $P < 0.05$ and ** $P < 0.01$ compared with corresponding non-irradiated HPBLs at 6 or 24 h post irradiation; ### $P < 0.01$ compared with corresponding HPBLs exposed to 0.5 Gy X-ray at 24 h post irradiation.

induced pan-nuclear p-ATM and p-DNA-PKcs responses are also presented in the apoptotic HPBLs. Moreover, ATM/DNA-PKcs inhibitor KU55933 not only inhibited X-irradiation-induced p-ATM and p-DNA-PKcs foci and the pan-nuclear p-ATM and p-DNA-PKcs responses but also suppressed the pan-nuclear γ H2AX response and apoptosis in resting HPBLs. DNA-PK can be strongly activated

during apoptotic DNA fragmentation²⁴ and ATM also can be activated by small double-stranded DNA fragments.⁵⁰ Our results suggest that the pan-nuclear γ H2AX response is triggered by transient pan-nuclear p-ATM and p-DNA-PKcs signals in resting HPBLs, and that the pan-nuclear γ H2AX response has a key role in X-ray-induced apoptosis in resting HPBLs.

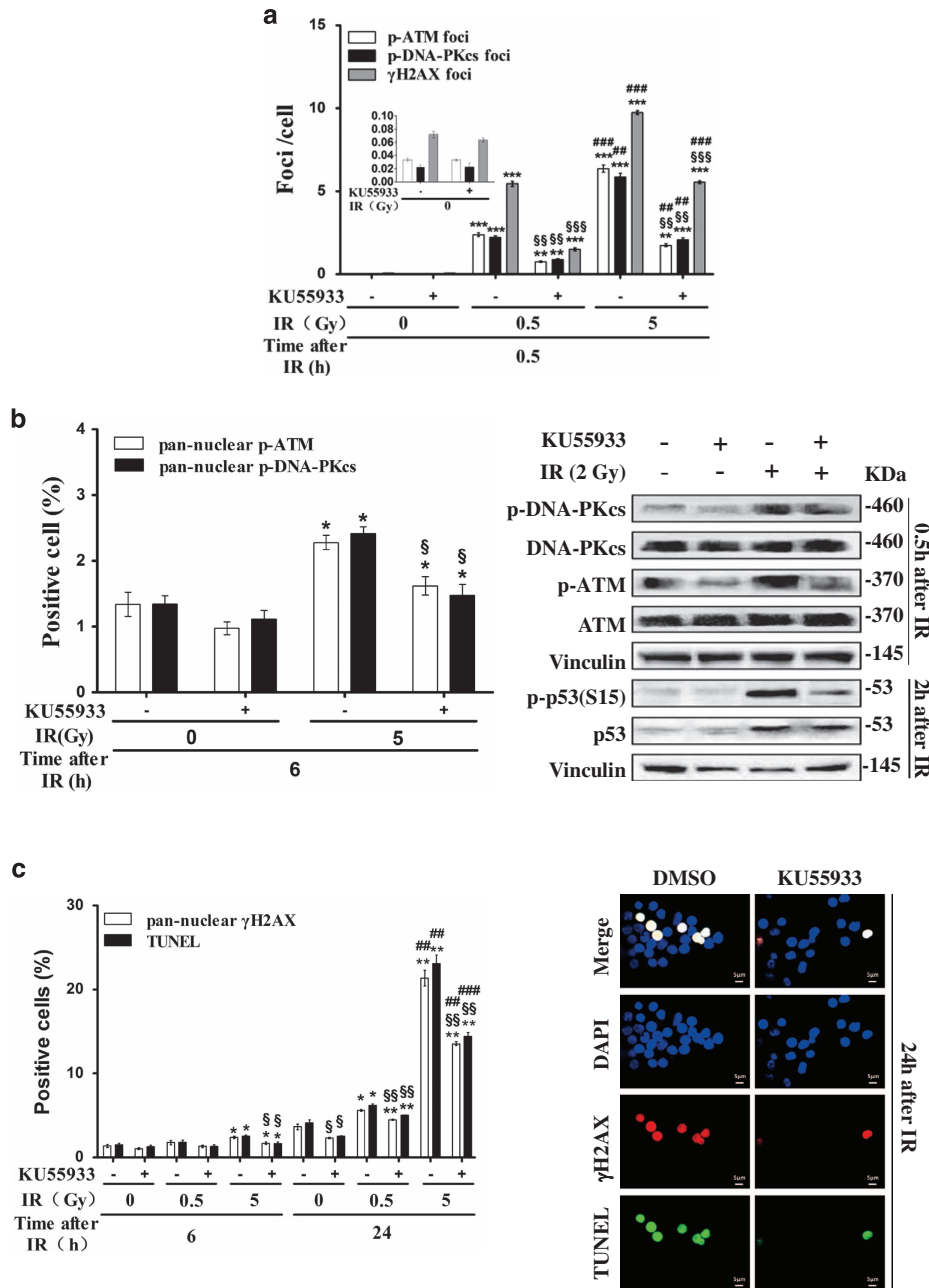


Figure 3. Inhibition of X-irradiation-induced pan-nuclear γ H2AX response and apoptosis in resting HPBLs by KU55933. **(a)** HPBLs were treated with 10 μ M KU55933 for 2 h before X-irradiation (0.5 or 5 Gy). γ H2AX, p-ATM and p-DNA-PKcs foci were measured in 500–1000 HPBLs from each sample. **(b)** HPBLs were treated with 10 μ M KU55933 for 2 h before X-irradiation (5 Gy). Pan-nuclear p-ATM and p-DNA-PKcs cells (left panel) were counted, and western blotting assays (right panel) were performed to examine the expression of p-ATM/ATM, p-DNA-PKcs/DNA-PKcs and p-p53/p53 proteins at the indicated time points after irradiation. **(c)** HPBLs were treated with 10 μ M KU55933 for 2 h before X-irradiation (0.5 or 5 Gy). Pan-nuclear γ H2AX and TUNEL-positive cells were measured, and their representative images were captured at 24 h after X-irradiation; γ H2AX was labeled in red and TUNEL in green, and nuclei were stained in blue with DAPI. A total of 2000–5000 HPBLs from each sample were examined to determine the percentage of the pan-nuclear γ H2AX, p-ATM, p-DNA-PKcs and TUNEL-positive cells. $\times 100$ magnification, $\times 1.0$ zoom. The values shown in panel **(a)**, panel **(b)** and panel **(c)** represent the means \pm S.D. obtained from three to four donors. * $P < 0.05$, ** $P < 0.01$ and *** $P < 0.001$ compared with corresponding non-irradiated HPBLs; ## $P < 0.01$ and ### $P < 0.001$ compared with corresponding HPBLs exposed to 0.5 Gy X-ray irradiation with/without inhibitor treatment; $^{\$}P < 0.05$, $^{\$\$}P < 0.01$ and $^{\$ \$ \$}P < 0.001$ compared with corresponding HPBLs without inhibitor treatment.

γ H2AX was recently shown to be a crucial component in modulating apoptosis.^{18,51} Lu *et al.*⁵¹ showed that H2AX S139 phosphorylation by ultraviolet A-activated c-Jun N-terminal kinase (JNK) is required for DNA ladder formation mediated by caspase-3/caspase-activated DNase (CAD) in apoptotic cells. Cook *et al.*¹⁸ reported that phosphorylation of tyrosine 142 of H2AX promoted the apoptotic response and inhibited the DDR to DNA damage.

When H2AX tyrosine 142 was mutated to alanine, only γ H2AX foci, but not pan-nuclear γ H2AX and TUNEL staining, occurred after irradiation in H2AX^{-/-} mouse embryonic fibroblast cells transfected with mutant H2AX (Y142F).¹⁸ These observations support our results that X-irradiation-induced pan-nuclear γ H2AX is involved in X-irradiation-induced apoptosis in resting HPBLs. Our results also suggest that there are no H2AX mutations at S139 and

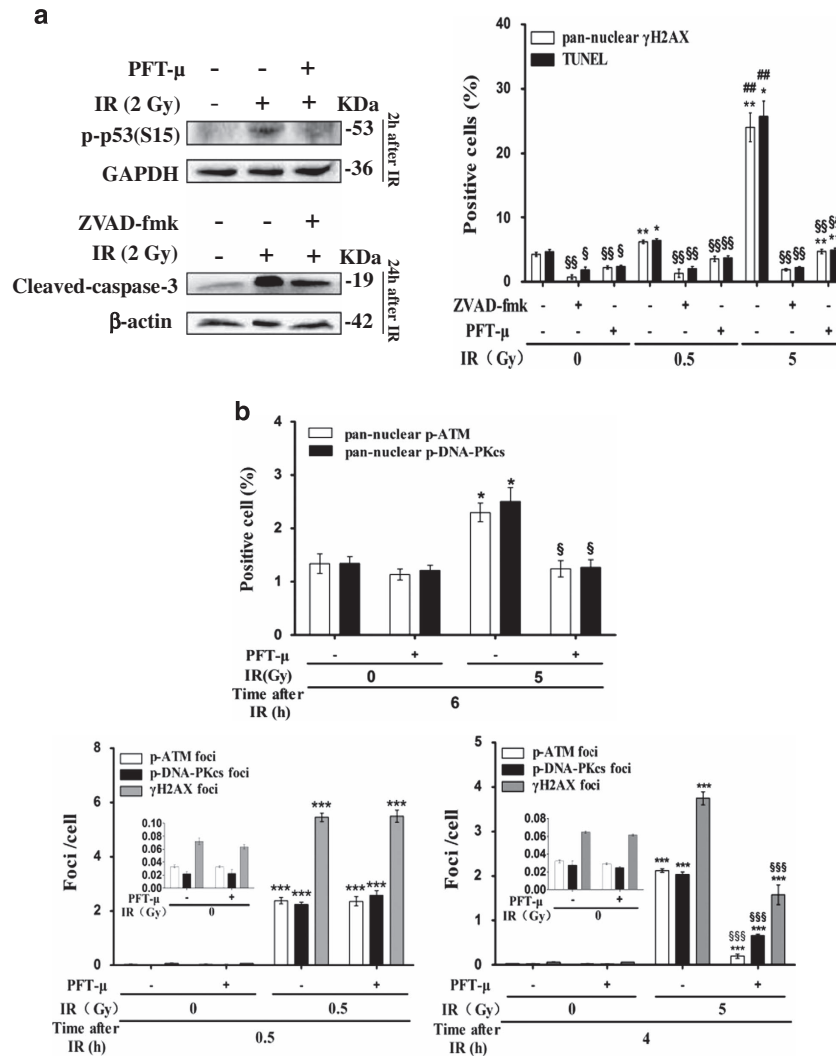


Figure 4. Inhibition of X-irradiation-induced pan-nuclear γ H2AX response and apoptosis in resting HPBLs by PFT- μ and ZVAD-fmk. **(a)** HPBLs were treated with 20 μ M PFT- μ for 5 h or 100 μ M ZVAD-fmk for 1 h before X-irradiation (2 Gy). The levels of p-p53 expression (left upper panel) and cleaved caspase-3 expression (left bottom panel) in HPBLs at indicated time points post irradiation were examined by western blotting. Furthermore, pan-nuclear γ H2AX and TUNEL-positive cells were counted at 24 h post irradiation. **(b)** HPBLs was treated with 20 μ M PFT- μ for 5 h before X-irradiation. Pan-nuclear p-ATM- and p-DNA-PKcs-positive cells were counted at 6 h post irradiation (upper panel). γ H2AX, p-ATM and p-DNA-PKcs foci were measured in HPBLs at 0.5 h (left bottom panel) and 4 h (right bottom panel) post irradiation. A total of 1000 HPBLs from each sample were examined for quantitation of the p-ATM, p-DNA-PKcs and γ H2AX foci, and 2000–5000 HPBLs from each sample were examined to calculate the percentage of pan-nuclear γ H2AX, p-ATM, p-DNA-PKcs and TUNEL-positive cells. The values shown in panel **(a)** and panel **(b)** represent the means \pm S.D. obtained from three to four donors. * $P < 0.05$, ** $P < 0.01$ and *** $P < 0.001$ compared with corresponding non-irradiated HPBLs with/without inhibitor treatment; ## $P < 0.01$ compared with corresponding HPBLs exposed to 0.5 Gy X-ray irradiation with/without inhibitor treatment; $^{\$}P < 0.05$, $^{\$\$}P < 0.01$ and $^{\$ \$ \$}P < 0.01$ compared with corresponding HPBLs without inhibitor treatment.

Y142 sites in HPBLs, and that pan-nuclear γ H2AX staining can be used to detect the apoptosis of HPBLs exposed to low LET IR. In addition, no γ H2AX, p-ATM and p-DNA-PKcs foci were observed in the X-ray-induced pan-nuclear response and TUNEL-positive HPBLs. One possible explanation is that the condensed chromatin in the late stages of apoptosis blocks the expression of DNA repair proteins.¹⁹ All together, we proposed that γ H2AX regulates apoptosis in a pan-nuclear response pattern and is involved in the DSB repair response in a focal pattern in resting HPBLs.

It has been reported that IR-induced HPBLs apoptosis is mediated by caspase cascade and is p53-dependent,^{42–47} which raises a question of whether X-irradiation-induced pan-nuclear γ H2AX response is also dependent on p53 and caspases. In the present study, we demonstrated that p53 inhibitor PFT- μ and caspase inhibitor ZVAD-fmk inhibited the X-irradiation-induced nuclear-wide γ H2AX response and apoptosis. A possible

explanation is that the pan-nuclear γ H2AX response is involved in the initiation and execution of apoptosis in HPBLs, and that p53 and caspases mediate the pan-nuclear γ H2AX response by priming and executing apoptosis, respectively. Coincident with the inhibition of X-irradiation-induced pan-nuclear γ H2AX response, we found that p53 inhibitor PFT- μ decreased the X-irradiation-induced pan-nuclear p-ATM and p-DNA-PKcs responses, suggesting that p53 may mediate the pan-nuclear γ H2AX response through activating the pan-nuclear p-ATM and p-DNA-PKcs responses. It has been found that wild-type p53 protein is able to rejoin DNA with DSBs to facilitate precise ligation through direct physical interaction of p53 with DNA-PK of NHEJ,^{52–54} and that p53 phosphorylation by ATM is involved in the initial steps of DNA damage signaling.⁵⁵ In the present study, we also demonstrated that p53 inhibition by PFT- μ results in a decrease of DSB repair and an increase of chromosome breaks by

inhibiting the X-irradiation-induced p-ATM and p-DNA-PKcs focus formation. Similar to ATM/DNA-PKcs inhibitor KU55933, PFT- μ can inhibit the pan-nuclear γ H2AX response, the formation of p-ATM and p-DNA-PKcs foci, and pan-nuclear p-ATM and p-DNA-PKcs responses. However, we also found that caspase inhibitor ZVAD-fmk decreased the nuclear-wide γ H2AX response and apoptosis but did not affect the X-ray-induced chromosome breaks,

suggesting that the nuclear-wide γ H2AX response is involved in caspase-mediated apoptotic execution, but caspases are not involved in DSB repair, as caspases are activated at the execution phase of apoptosis when DSB repair process is finished.

It is well established that the IR-induced massive cell death in radiosensitive tissues is not due to irreversible damage of cells but rather to activation of apoptosis, therefore blockage of apoptosis has become a pharmacological approach to radioprotection of normal tissues.⁵⁶ Similarly, inhibition of DSB repair has been well known as an efficient approach to facilitate the apoptosis and sensitize tumor cells to IR and DSB-inducing chemotherapeutic agents such as etoposide, doxorubicin and camptothecin.⁵⁷ Surprisingly, we found that ATM/DNA-PKcs inhibitor KU55933 protected resting HPBLs from the X-ray-induced pan-nuclear γ H2AX response and apoptosis, although it inhibited the X-ray-induced DSBs repair and enhanced chromosomal breaks. Our results are consistent with the literature reports that inhibition of ATM and DNA-PKcs phosphorylation by KU55933 can result in the suppression of H2AX phosphorylation and etoposide-induced apoptosis in resting HPBLs.^{26,58} It is believed that HPBLs in a resting status tolerate a limited un-repair and inaccurate repair, and that there are opposite actions of KU55933 on normal resting cells and proliferating cancer cells. Owing to dual functions of p53 in mediating the DSB repair and apoptosis in resting HPBLs, p53 inhibitor PFT- μ , like ATM/DNA-PKcs inhibitor KU55933, protected resting HPBLs from the X-ray-induced pan-nuclear γ H2AX response and apoptosis, and concurrently induced a decrease of DSB repair and an increase of chromosome breaks and frequencies of chromosomal aberrations. Our observations are consistent with the findings that PFT- α decreases the repair efficiency of X-ray-induced DNA lesions, leading to increased frequencies of chromosomal aberrations and reduced apoptosis in HPBLs.⁴⁶ Unlike the dual role of KU55933 and PFT- μ , caspase

Table 1. Effects of KU55933, PFT- μ and ZVAD-fmk on frequencies of X-irradiation-induced chromosomal aberrations at 48 h post irradiation in resting HPBLs

Treatment	Chromosomal aberrations/100 cells		% Aberrant cells
	Breaks	Dicentric+rings	
Ctrl	0.7 \pm 0.3	0.5 \pm 0.5	1.2 \pm 0.8
KU55933	0.7 \pm 0.6	0	0.7 \pm 0.6
PFT- μ	0	0	0
ZVAD-fmk	0.3 \pm 0.6	0	0.3 \pm 0.6
IR	13.8 \pm 2.5**	14.1 \pm 2.2**	21.3 \pm 3.3**
KU55933+IR	24.2 \pm 2.3** ^{§§}	23.7 \pm 3.7*** [§]	40.7 \pm 5.0*** ^{§§}
PFT- μ +IR	22.3 \pm 2.4*** [§]	20.7 \pm 2.8** [§]	34.7 \pm 2.4*** ^{§§}
ZVAD-fmk+IR	17.9 \pm 5.8*	13.5 \pm 4.9*	25.6 \pm 4.8**

Resting HPBLs were pretreated with 10 μ M KU55933 for 2 h, 20 μ M PFT- μ for 5 h or 100 μ M ZVAD-fmk for 1 h followed by irradiation with 2 Gy X-rays, and incubated with PHA and colcemid for 48 h. The metaphase cells were then harvested, and a total of 100 metaphase cells were analyzed. The values represent the means \pm S.D. of HPBLs from three individual donors. * P < 0.05, ** P < 0.01 and *** P < 0.001, compared with non-irradiated control and inhibitor treatment alone; [§] P < 0.05 and ^{§§} P < 0.01, compared with IR alone.

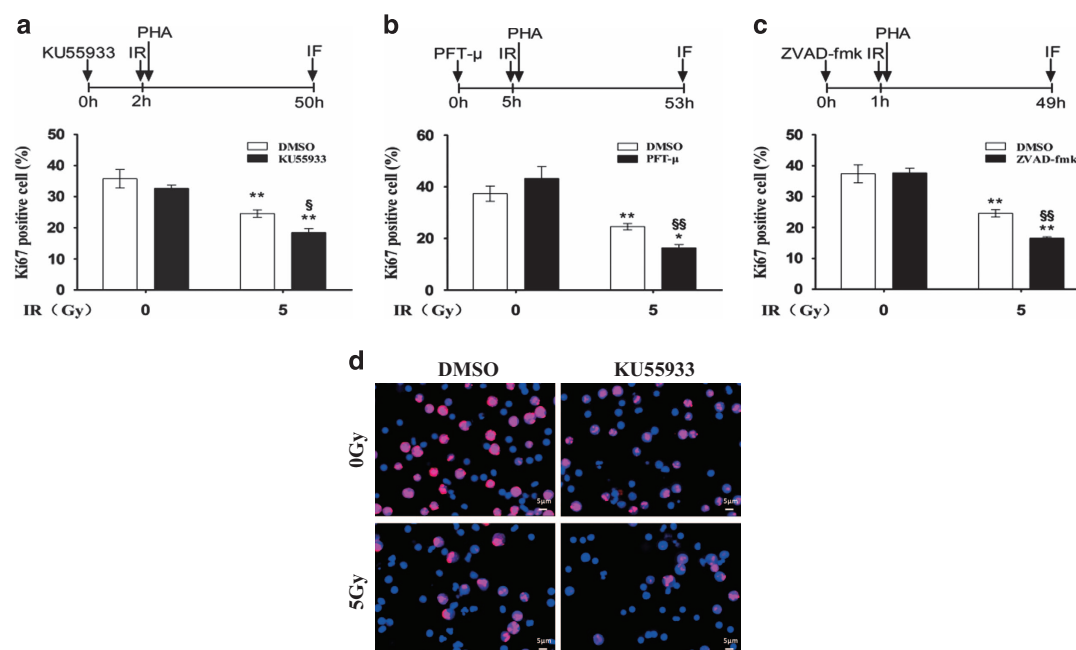


Figure 5. KU55933, PFT- μ and ZVAD-fmk inhibited the proliferative response to mitogen in resting HPBLs exposed to X-ray irradiation. HPBLs were treated with 10 μ M KU55933 for 2 h (**a**), 20 μ M PFT- μ for 5 h (**b**) or 100 μ M ZVAD-fmk for 1 h (**c**) followed by irradiation with 5 Gy X-ray, and were cultured with PHA and colcemid for 48 h. HPBLs were then collected and transformed HPBLs were detected using the Ki67 antibody. A total of 1000 HPBLs from each sample were examined to determine the proliferation ratio. Data are presented as the means \pm S.D. obtained from three donors. * P < 0.05 and ** P < 0.01 compared with corresponding non-irradiated HPBLs with/without inhibitor treatment; [§] P < 0.05 and ^{§§} P < 0.01 compared with corresponding HPBLs without inhibitor treatment. (**d**) Representative images of HPBLs labeled with Ki67. The cells were treated with KU55933 and irradiated with X-ray as described above. Ki67 was labeled in red and nuclei were stained in blue with DAPI. \times 40 magnification, \times 1.0 zoom.

inhibitor ZVAD-fmk protected HPBLs from X-ray-induced nuclear-wide γ H2AX response and apoptosis, and did not worsen the X-ray-induced chromosomal instability. More importantly, we found that the inhibition of X-ray-induced nuclear-wide γ H2AX response and apoptosis by KU55933, PFT- μ and ZVAD-fmk aggravated the inhibitory effects of X-irradiation on the proliferative response of HPBLs to mitogens, suggesting that the inhibition of the nuclear-wide γ H2AX response and apoptosis does not protect the function of HPBLs. It is possible that the inhibition of DSB repair by KU55933 and PFT- μ does not result in correction of chromosome aberrations in HPBLs, and that the increased genomic instability leads to further suppression of the proliferative response of HPBLs exposed to X-irradiation, which limits the pharmacological use of DSB repair inhibitors and p53 inhibitors in radioprotection of normal tissues. Nevertheless, the aggravated effect of ZVAD-fmk on IR-induced proliferative inhibition may be related to suppression of the expression of lymphocyte-stimulated factor receptors, such as IL-2.⁵⁹ Lawrence *et al.*⁵⁹ found that ZVAD-fmk inhibits the proliferative response of human T lymphocytes induced by mitogens and IL-2 via inhibiting the expression of the IL-2 receptor, and that suppression of human T-cell proliferation by ZVAD-fmk is independent of its caspase inhibition properties, as ZVAD-fmk inhibits caspase processing during apoptosis but not during T-cell activation. Because caspase inhibitors are capable of providing reversible inhibitory effects on proliferative response in HPBLs by temporarily blocking the expression of proliferative response receptors, we proposed that inhibition of caspases would be a promising pharmacological approach for radio-protection of HPBLs.

In summary, we showed herein that X-irradiation induced not only the pan-nuclear γ H2AX response but also the transient pan-nuclear p-ATM and p-DNA-PKcs responses in addition to the formation of nuclear DDR foci containing activated ATM, DNA-PKcs and γ H2AX in resting HPBLs. The pan-nuclear γ H2AX response and the transient pan-nuclear p-ATM and p-DNA-PKcs responses were directly related to X-ray-induced apoptosis. Moreover, the pan-nuclear γ H2AX response and apoptosis were mediated not only by transient pan-nuclear p-ATM and p-DNA-PKcs signals but also by p53 and pan-caspase activities in resting HPBLs exposed to X-irradiation. ATM/DNA-PKcs inhibitor and p53 inhibitor attenuate the X-ray-induced pan-nuclear γ H2AX response and apoptosis, but worsen the X-ray-induced functional impairment and genomic instability, suggesting that these inhibitors cannot be used as radioprotective agents for HPBLs. The pan-caspase inhibitor attenuates X-ray-induced pan-nuclear γ H2AX response and apoptosis with no effect on X-ray-induced genomic instability and holds developmental promise.

MATERIALS AND METHODS

Peripheral blood sample collection and lymphocyte isolation and culture

Human peripheral blood samples were obtained from informed healthy male and female volunteers (22–25 years old), and the research was approved by Fudan University School of Public Health Institutional Review Board. For each experiment, blood was collected in sterile heparinized Vacutainers from three to six different donors. Lymphocytes were isolated from blood using density gradient centrifugation in Ficoll-Paque (Cedarlane Co., Burlington, ON, Canada) according to the manufacturer's instructions. Isolated HPBLs at a density of 1×10^6 cell/ml were cultured in RPMI 1640 medium (Gibco, Invitrogen Technologies, Carlsbad, CA, USA) supplemented with 15% fetal calf serum (Invitrogen Technologies), 5% (v/v) plasma, 100 U/ml penicillin and 100 μ g/ml streptomycin at 5% CO₂ and 37°C in a humidified incubator. The viability of the isolated HPBLs was above 95% as measured with the trypan blue exclusion assay.

Irradiation and treatment

An X-Rad 320 biological irradiator (Precision X-Ray, Inc., North Branford, CT, USA) was used for the X-ray irradiation, and the dose rate was 1.83 Gy/min. The HPBLs were pretreated with 10 μ M KU55933 (Selleckchem, Houston, TX, USA) for 2 h, 20 μ M PFT- μ (Selleckchem) for 5 h or 100 μ M ZVAD-fmk (Selleckchem) for 1 h, and then irradiated in a flask at room temperature at doses of 0.5, 2 or 5 Gy. After irradiation, the cells were incubated in a CO₂ incubator at 37°C and harvested after various repair periods for immunofluorescence staining, apoptosis assay and western blotting analysis. For the lymphocyte proliferative assay, phytohemagglutinin (Shanghai Jikong Biotechnology, Shanghai, China) was added to the culture medium after IR, and the cells were further incubated for 48 h.

Immunofluorescence analysis

The suspension of irradiated and sham-irradiated HPBLs was immediately placed on ice for 10 min and washed in ice-cold PBS, and the cells were spun onto the triple chambered slides precoated with 50 mg/l poly-L-lysine (Sigma, St. Louis, MO, USA) using a cytospin centrifuge (Iris sample processing, Beckman Coulter Inc., Miami, FL, USA), fixed with 4% paraformaldehyde for 15 min, permeabilized with 0.5% Triton X-100 for 15 min and followed by blocking with 10% (v/v) fetal calf serum in PBS at 37°C for 1 h. The cells were then incubated overnight at 4°C with anti- γ H2AX (S139) antibody (Cell Signaling Technology, Danvers, MA, USA), anti-phospho-ATM (S1981) antibody (Abcam, Hong Kong, China) and anti-phospho-DNA-PKcs (T2609) antibody (Abcam) or anti-Ki67 antibody (Cell Signaling Technology), followed by secondary antibody labeled with Alexa Fluor 488-conjugated donkey anti-rabbit (Molecular probe, Life Technologies, Grand Island, NY, USA), Alexa Fluor 555-conjugated donkey anti-mouse or Alexa Fluor 647-conjugated donkey anti-rabbit (Molecular probe) at room temperature for 1 h. Fluorescence images were acquired by an Olympus BX51 fluorescent microscope (Olympus Optical Co., Tokyo, Japan) equipped with a COHU CCD camera (Audio Video Supply, San Diego, CA, USA) and VideoTesT-FISH software (VideoTesT, Saint Petersburg, Russia). Images used for comparisons between different treatments were acquired and processed with the same instrument settings. The normalized levels of pan-nuclear staining or foci of γ H2AX, p-ATM (S1981) and p-DNA-PKcs (T2609) were the ratios of the number of pan-nuclear staining or foci to the number of cells scored. In addition, colocalization of TUNEL staining with pan-nuclear γ H2AX, p-ATM or p-DNA-PKcs staining, and colocalization of pan-nuclear γ H2AX staining with pan-nuclear p-ATM or p-DNA-PKcs staining were examined. The colocalization ratios were calculated as follows: number of colocalized pan-nuclear staining/number of TUNEL staining or pan-nuclear γ H2AX staining.

Apoptosis detection

After pretreatment with inhibitors of ATM/DNA-PKcs, p53 and pan-caspases or/and X-irradiation, the cell monolayers were spun down on slides, and subjected to terminal deoxynucleotidyl transferase-mediated dUTP (2'-deoxyuridine 5'-triphosphate) biotin nick end labeling (TUNEL) staining using a TUNEL Apoptosis Detection Kit (Vazyme Biotech, Nanjing, Jiangsu Province, China) for *in situ* detection of apoptosis according to the manufacturer's instructions. For combination with immunofluorescence analysis, fluorescein isothiocyanate-12-dUTP labeling mix was added and incubated for 1 h after incubation with the primary antibody, followed by incubation with the secondary antibody. The TUNEL-stained cells were counter-stained with mounting medium containing 4',6-diamidino-2-phenylindole (DAPI) (Santa Cruz Biotechnology, Santa Cruz, CA, USA); the fluorescein isothiocyanate-labeled TUNEL-positive cells were imaged using an Olympus BX51 fluorescent microscope, and the TUNEL-positive cells were counted to calculate the TUNEL indices.

Chromosomal aberration analysis

After pretreatment with inhibitors of ATM/DNA-PKcs, p53 and pan-caspases, HPBLs were irradiated by X-rays. After a 2-h repair period, the cells were incubated with colcemid and phytohemagglutinin, and the levels of X-ray-induced chromosomal aberrations in HPBLs were determined at 48 h after irradiation. Chromosome preparations were made using standard techniques after the incubation of the cells in hypotonic solution (0.075 M KCl) and fixation with methanol/acetic acid (3:1). For each sample, 100 metaphases per donor were scored. The chromosomal aberrations were classified according to Savage.⁶⁰

Western blotting

Cell extracts were prepared in radioimmunoprecipitation assay buffer containing 1% (v/v) proteinase inhibitor, 1% (v/v) phosphatase inhibitor cocktail, 1 mM phenylmethylsulfonyl fluoride and 1 mM sodium orthovanadate. Aliquots (60 μ g protein) from each sample were loaded into each lane of sodium dodecyl sulfate-polyacrylamide gel electrophoresis gels and subjected to gel electrophoresis, and followed by transfer to polyvinylidene fluoride membranes (Millipore, Bedford, MA, USA). The membranes were incubated overnight at 4 °C with the primary anti- γ H2AX (S139) antibody (1 : 1000) (Cell Signaling Technology), anti-phospho-ATM (S1981) antibody (1 : 1000) (Abcam), anti-ATM antibody (1 : 500) (Santa Cruz), anti-phospho-DNA-PKcs (T2609) antibody (1 : 1000) (Abcam), anti-DNA-PKcs antibody (1 : 500) (Santa Cruz), anti-phospho-p53 (S15) antibody (1 : 1000) (Cell Signaling Technology), anti-p53 antibody (1 : 500) (Santa Cruz) or anti-cleaved-caspase-3 antibody (1 : 1000) (Cell Signaling Technology). The membranes were then incubated for 1 h at room temperature with the secondary antibody: IgG-HRP antibody (1 : 2500) (Immunology Consultants Laboratory, Inc., Portland, OR, USA). Enhanced chemiluminescence was then performed (ECL Kit, Millipore) according to the manufacturer's protocol. The densitometry analysis was performed with the ChemiDoc detection system (Bio-Rad Laboratories, Hercules, CA, USA) and Quantity One software (Bio-Rad). The membranes were also probed with anti-GAPDH antibody (1 : 1000) (Huaan Biotechnology, Hangzhou, Zhejiang Province, China), anti- β -actin antibody (1 : 5000) (Huaan Biotechnology) or anti-vinculin antibody (1 : 10000) (Abcam) as the internal control.

Statistical analysis

Data are presented as the means \pm standard deviation. Statistical analysis of the data was performed using SPSS 17.0 software. Independent-samples *T* test was applied to analyze the differences. A difference with *P* < 0.05 was considered to be statistically significant.

ABBREVIATIONS

HPBLs, human peripheral blood lymphocytes; IR, ionizing radiation; γ H2AX, Phosphorylated histone variant H2AX; dUTP, 2'-deoxyuridine 5'-triphosphate; TUNEL, terminal deoxynucleotidyl transferase-mediated dUTP biotin nick end labeling; LET, linear energy transfer; p-ATM, phosphorylated Ataxia telangiectasia mutated; p-DNA-PKcs, phosphorylated DNA-dependent protein kinase catalytic subunit; ATM, Ataxia telangiectasia mutated; DNA-PKcs, DNA-dependent protein kinase catalytic subunit; PFT- μ , Pifithrin- μ ; PFT- α , Pifithrin- α ; DSBs, double strand breaks; DDR, DNA damage response; TRAIL, tumor necrosis factor-related apoptosis-inducing ligand; JNK, c-Jun N-terminal kinase; CAD, caspase-3/caspase-activated DNase; NHEJ, non-homologous end-joining; IL-2, Interleukin-2; RPMI, Roswell Park Memorial Institute; PHA, phytohemagglutinin; PBS, phosphate-buffered saline; DAPI, 4',6-diamidino-2-phenylindole; S.D., standard deviation.

ACKNOWLEDGEMENTS

We thank Meijun Zhou for chromosome aberration analysis; Advanced Research Scientist Yonghe Li of Department of Biochemistry and Molecular Biology, Southern Research Institute in Birmingham for manuscript editing. This work was supported by the National Nature Science Foundation of China (81273000, 31370839).

AUTHOR CONTRIBUTIONS

DF performed experiments, analyzed data, designed figures and wrote the manuscript; YZ, JW, XZ, YG, LY and QL performed experiments; JL interpreted data; and HC designed the research, supervised the study, designed figures, analyzed the data and wrote the manuscript.

COMPETING INTERESTS

The authors declare no conflict of interest.

REFERENCES

1 Jackson SP, Bartek J. The DNA-damage response in human biology and disease. *Nature* 2009; **461**: 1071–1078.

- Rogakou EP, Boon C, Redon C, Bonner WM. Megabase chromatin domains involved in DNA double-strand breaks in vivo. *J Cell Biol* 1999; **146**: 905–915.
- Rogakou EP, Pilch DR, Orr AH, Ivanova VS, Bonner WM. DNA double-stranded breaks induce histone H2AX phosphorylation on serine 139. *J Biol Chem* 1998; **273**: 5858–5868.
- Burma S, Chen BP, Murphy M, Kurimasa A, Chen DJ. ATM phosphorylates histone H2AX in response to DNA double-strand breaks. *J Biol Chem* 2001; **276**: 42462–42467.
- Stiff T, O'Driscoll M, Rief N, Iwabuchi K, Lobrich M, Jeggo PA. ATM and DNA-PK function redundantly to phosphorylate H2AX after exposure to ionizing radiation. *Cancer Res* 2004; **64**: 2390–2396.
- Wang H, Wang M, Wang H, Bocker W, Iliakis G. Complex H2AX phosphorylation patterns by multiple kinases including ATM and DNA-PK in human cells exposed to ionizing radiation and treated with kinase inhibitors. *J Cell Physiol* 2005; **202**: 492–502.
- Lane DP. Cancer - P53, guardian of the genome. *Nature* 1992; **358**: 15–16.
- Canman CE, Lim DS, Cimprich KA, Taya Y, Tamai K, Sakaguchi K *et al*. Activation of the ATM kinase by ionizing radiation and phosphorylation of p53. *Science* 1998; **281**: 1677–1679.
- Rathmell WK, Kaufmann WK, Hurt JC, Byrd LL, Chu G. DNA-dependent protein kinase is not required for accumulation of p53 or cell cycle arrest after DNA damage. *Cancer Res* 1997; **57**: 68–74.
- Jimenez GS, Bryntesson F, Torres-Arzuay MI, Priestley A, Beeche M, Saito Si *et al*. DNA-dependent protein kinase is not required for the p53-dependent response to DNA damage. *Nature* 1999; **400**: 81–83.
- Jhappan C, Yusufzai TM, Anderson S, Anver MR, Merlino G. The p53 response to DNA damage in vivo is independent of DNA-dependent protein kinase. *Mol Cell Biol* 2000; **20**: 4075–4083.
- Wang S, Guo M, Ouyang H, Li XL, Cordon-Cardo C, Kurimasa A *et al*. The catalytic subunit of DNA-dependent protein kinase selectively regulates p53-dependent apoptosis but not cell-cycle arrest. *Proc Natl Acad Sci USA* 2000; **97**: 1584–1588.
- Callen E, Jankovic M, Wong N, Zha S, Chen HT, Difilippantonio S *et al*. Essential role for DNA-PKcs in DNA double-strand break repair and apoptosis in ATM-deficient lymphocytes. *Mol Cell* 2009; **34**: 285–297.
- Sengupta S, Harris CC. p53: traffic cop at the crossroads of DNA repair and recombination. *Nat Rev Mol Cell Biol* 2005; **6**: 44–55.
- Ding HF, Lin YL, McGill G, Joo P, Zhu H, Blenis J *et al*. Essential role for caspase-8 in transcription-independent apoptosis triggered by p53. *J Biol Chem* 2000; **275**: 38905–38911.
- Mihara M, Erster S, Zaika A, Petrenko O, Chittenden T, Pancoska P *et al*. p53 has a direct apoptogenic role at the mitochondria. *Mol Cell* 2003; **11**: 577–590.
- Leist M, Jaattela M. Four deaths and a funeral: From caspases to alternative mechanisms. *Nat Rev Mol Cell Bio* 2001; **2**: 589–598.
- Cook PJ, Ju BG, Telesse F, Wang X, Glass CK, Rosenfeld MG. Tyrosine dephosphorylation of H2AX modulates apoptosis and survival decisions. *Nature* 2009; **458**: 591–596.
- Markova E, Torudd J, Belyaev I. Long time persistence of residual 53BP1/gamma-H2AX foci in human lymphocytes in relationship to apoptosis, chromatin condensation and biological dosimetry. *Int J Radiat Biol* 2011; **87**: 736–745.
- Meyer B, Voss KO, Tobias F, Jakob B, Durante M, Taucher-Scholz G. Clustered DNA damage induces pan-nuclear H2AX phosphorylation mediated by ATM and DNA-PK. *Nucleic Acids Res* 2013; **41**: 6109–6118.
- Psonka-Antonczyk K, Elsasser T, Gudowska-Nowak E, Taucher-Scholz G. Distribution of double-strand breaks induced by ionizing radiation at the level of single DNA molecules examined by atomic force microscopy. *Radiat Res* 2009; **172**: 288–295.
- Solier S, Sordet O, Kohn KW, Pommier Y. Death receptor-induced activation of the Chk2- and histone H2AX-associated DNA damage response pathways. *Mol Cell Biol* 2009; **29**: 68–82.
- Rogakou EP, Nieves-Neira W, Boon C, Pommier Y, Bonner WM. Initiation of DNA fragmentation during apoptosis induces phosphorylation of H2AX histone at serine 139. *J Biol Chem* 2000; **275**: 9390–9395.
- Mukherjee B, Kessinger C, Kobayashi J, Chen BP, Chen DJ, Chatterjee A *et al*. DNA-PK phosphorylates histone H2AX during apoptotic DNA fragmentation in mammalian cells. *DNA Repair (Amst)* 2006; **5**: 575–590.
- de Feraudy S, Revet I, Bezrookove V, Feeney L, Cleaver JE. A minority of foci or pan-nuclear apoptotic staining of gammaH2AX in the S phase after UV damage contain DNA double-strand breaks. *Proc Natl Acad Sci USA* 2010; **107**: 6870–6875.
- Korwek Z, Sewastianik T, Bielak-Zmijewska A, Mosieniak G, Alster O, Moreno-Villanueva M *et al*. Inhibition of ATM blocks the etoposide-induced DNA damage response and apoptosis of resting human T cells. *DNA Repair (Amst)* 2012; **11**: 864–873.
- Furuta T, Hayward R, Meng L, Takemura H, Aune G, Bonner W *et al*. p21CDKN1A allows the repair of replication-mediated DNA double-strand breaks induced by

- topoisomerase I and is inactivated by the checkpoint kinase inhibitor 7-hydroxystaurosporine. *Oncogene* 2006; **25**: 2839–2849.
- 28 Antony S, Agama KK, Miao ZH, Takagi K, Wright MH, Robles AI et al. Novel indenoisoquinolines NSC 725776 and NSC 724998 produce persistent topoisomerase I cleavage complexes and overcome multidrug resistance. *Cancer Res* 2007; **67**: 10397–10405.
- 29 Ewald B, Sampath D, Plunkett W. H2AX phosphorylation marks gemcitabine-induced stalled replication forks and their collapse upon S-phase checkpoint abrogation. *Mol Cancer Ther* 2007; **6**: 1239–1248.
- 30 Quanz M, Berthault N, Roulin C, Roy M, Herbette A, Agrario C et al. Small-molecule drugs mimicking DNA damage: a new strategy for sensitizing tumors to radiotherapy. *Clin Cancer Res* 2009; **15**: 1308–1316.
- 31 Quanz M, Chassoux D, Berthault N, Agrario C, Sun JS, Dutreix M. Hyperactivation of DNA-PK by double-strand break mimicking molecules disorganizes DNA damage response. *Plos One* 2009; **4**: e6298.
- 32 Fragkos M, Breuleux M, Clement N, Beard P. Recombinant adeno-associated viral vectors are deficient in provoking a DNA damage response. *J Virol* 2008; **82**: 7379–7387.
- 33 Schwartz RA, Carson CT, Schubert C, Weitzman MD. Adeno-associated virus replication induces a DNA damage response coordinated by DNA-dependent protein kinase. *J Virol* 2009; **83**: 6269–6278.
- 34 Baure J, Izadi A, Suarez V, Giedzinski E, Cleaver JE, Fike JR et al. Histone H2AX phosphorylation in response to changes in chromatin structure induced by altered osmolarity. *Mutagenesis* 2009; **24**: 161–167.
- 35 IAEA. *Cytogenetic Analysis for Radiation Dose Assessment: A Manual*, IAEA (International Atomic Energy Agency) Technical Reports Series. No.405: Vienna, 2001.
- 36 Dikomey E, Borgmann K, Peacock J, Jung H. Why recent studies relating normal tissue response to individual radiosensitivity might have failed and how new studies should be performed. *Int J Radiat Oncol* 2003; **56**: 1194–1200.
- 37 Cogoli-Greuter M. The lymphocyte story - an overview of selected highlights on the in vitro activation of human lymphocytes in space. *Microgravity Sci Tec* 2014; **25**: 343–352.
- 38 Bui N, Saitakis M, Dogniaux S, Buschinger O, Bohneust A, Richert A et al. Human primary immune cells exhibit distinct mechanical properties that are modified by inflammation. *Biophys J* 2015; **108**: 2181–2190.
- 39 Rothkamm K, Lobrich M. Evidence for a lack of DNA double-strand break repair in human cells exposed to very low x-ray doses. *Proc Natl Acad Sci U S A* 2003; **100**: 5057–5062.
- 40 Bourton EC, Plowman PN, Smith D, Arlett CF, Parris CN. Prolonged expression of the gamma-H2AX DNA repair biomarker correlates with excess acute and chronic toxicity from radiotherapy treatment. *Int J Cancer* 2011; **129**: 2928–2934.
- 41 Kabacik S, Ortega-Molina A, Efeyan A, Finnon P, Bouffler S, Serrano M et al. A minimally invasive assay for individual assessment of the ATM/CHEK2/p53 pathway activity. *Cell Cycle* 2011; **10**: 1152–1161.
- 42 Shen Y, White E. p53-dependent apoptosis pathways. *Adv Cancer Res* 2001; **82**: 55–84.
- 43 Bassi L, Carloni M, Meschini R, Fonti E, Palitti F. X-irradiated human lymphocytes with unstable aberrations and their preferential elimination by p53/survivin-dependent apoptosis. *Int J Radiat Biol* 2003; **79**: 943–954.
- 44 Belloni P, Meschini R, Czene S, Harms-Ringdahl M, Palitti F. Studies on radiation-induced apoptosis in G0 human lymphocytes. *Int J Radiat Biol* 2005; **81**: 587–599.
- 45 Vilasova Z, Rezacova M, Vavrova J, Tichy A, Vokurkova D, Zoelzer F et al. Changes in phosphorylation of histone H2AX and p53 in response of peripheral blood lymphocytes to gamma irradiation. *Acta Biochim Pol* 2008; **55**: 381–390.
- 46 Meschini R, Berni A, Ortenzi V, Mancinelli P, Palitti F. Relation between DNA repair, apoptosis and chromosomal aberrations in presence of pifithrin- α , an inhibitor of p53. *Mutat Res* 2010; **701**: 92–97.
- 47 Yu YJ, Little JB. p53 is involved in but not required for ionizing radiation-induced caspase-3 activation and apoptosis in human lymphoblast cell lines. *Cancer Res* 1998; **58**: 4277–4281.
- 48 UNSCEAR. *Effects of Ionizing Radiation: Report to the General Assembly, with Scientific Annexes*, vol. 1: UNSCEAR (United Nations Scientific Committee on the Effects of Atomic Radiation): New York: United Nations, 2008.
- 49 ICRP. ICRP statement on tissue reactions/early and late effects of radiation in normal tissues and organs—threshold doses for tissue reactions in a radiation protection context. *ICRP (International Commission On Radiological Protection) Publication 118. Ann ICRP* vol. 41, 2012.
- 50 Shiotani B, Zou L. Single-stranded DNA orchestrates an ATM-to-ATR Switch at DNA Breaks. *Mol Cell* 2009; **33**: 547–558.
- 51 Lu C, Zhu F, Cho Y-Y, Tang F, Zykova T, Ma WY et al. Cell apoptosis: requirement of H2AX in DNA ladder formation, but not for the activation of caspase-3. *Mol Cell* 2006; **23**: 121–132.
- 52 Yang T, Namba H, Hara T, Takamura N, Nagayama Y, Fukata S et al. p53 induced by ionizing radiation mediates DNA end-jointing activity, but not apoptosis of thyroid cells. *Oncogene* 1997; **14**: 1511–1519.
- 53 Tang W, Willers H, Powell SN. p53 directly enhances rejoining of DNA double-strand breaks with cohesive ends in gamma-irradiated mouse fibroblasts. *Cancer Res* 1999; **59**: 2562–2565.
- 54 Lin Y, Waldman BC, Waldman AS. Suppression of high-fidelity double-strand break repair in mammalian chromosomes by pifithrin- α , a chemical inhibitor of p53. *DNA Repair (Amst)* 2003; **2**: 1–11.
- 55 Al Rashid ST, Delleire G, Cuddihy A, Jalali F, Vaid M, Coackley C et al. Evidence for the direct binding of phosphorylated p53 to sites of DNA breaks in vivo. *Cancer Res* 2005; **65**: 10810–10821.
- 56 Gudkov AV, Komarova EA. Radioprotection: smart games with death. *J Clin Invest* 2010; **120**: 2270–2273.
- 57 Hickson I, Zhao Y, Richardson CJ, Green SJ, Martin NM, Orr AI et al. Identification and characterization of a novel and specific inhibitor of the ataxia-telangiectasia mutated kinase ATM. *Cancer Res* 2004; **64**: 9152–9159.
- 58 Sordet O, Redon CE, Guirouilh-Barbat J, Smith S, Solier S, Douarre C et al. Ataxia telangiectasia mutated activation by transcription- and topoisomerase I-induced DNA double-strand breaks. *Embo Rep* 2009; **10**: 887–893.
- 59 Lawrence CP, Chow SC. Suppression of human T cell proliferation by the caspase inhibitors, z-VAD-FMK and z-IETD-FMK is independent of their caspase inhibition properties. *Toxicol Appl Pharmacol* 2012; **265**: 103–112.
- 60 Savage J. Classification and relationships of induced chromosomal structural changes. *J Med Genet* 1976; **13**: 103–122.



This work is licensed under a Creative Commons Attribution 4.0 International License. The images or other third party material in this article are included in the article's Creative Commons license, unless indicated otherwise in the credit line; if the material is not included under the Creative Commons license, users will need to obtain permission from the license holder to reproduce the material. To view a copy of this license, visit <http://creativecommons.org/licenses/by/4.0/>